Applied Microbiology and Biotechnology
https://doi.org/10.1007/s00253-022-12177-6

METHODS AND PROTOCOLS

An adaptive tracking illumination system for optogenetic control of single bacterial cells

Aiguo Xia[1] · Rongrong Zhang[2] · Yajia Huang[2] · Lei Ni[2] · Lu Pu[3] · Ye Li[1] · Shuai Yang[2] · Fan Jin[1,2]

Received: 26 May 2022 / Revised: 8 August 2022 / Accepted: 7 September 2022

Abstract

Single-cell behaviors are essential during early-stage biofilm formation. In this study, we aimed to evaluate whether single-cell behaviors could be precisely and continuously manipulated by optogenetics. We thus established adaptive tracking illumination (ATI), a novel illumination method to precisely manipulate the gene expression and bacterial behavior of *Pseudomonas aeruginosa* on the surface at the single-cell level by using the combination of a high-throughput bacterial tracking algorithm, optogenetic manipulation, and adaptive microscopy. ATI enables precise gene expression control by manipulating the optogenetic module gene expression and type IV pili (TFP)–mediated motility and microcolony formation during biofilm formation through bis-(3′-5′)-cyclic dimeric guanosine monophosphate (c-di-GMP) level modifications in single cells. Moreover, we showed that the spatial organization of single cells in mature biofilms could be controlled using ATI. Therefore, this novel method we established might markedly answer various questions or resolve problems in microbiology.

Key points

- *High-resolution spatial and continuous optogenetic control of individual bacteria.*
- *Phenotype-specific optogenetic control of individual bacteria.*
- *Capacity to control biologically relevant processes in engineered single cells.*

Keywords Adaptive microscopy · Optogenetics · *Pseudomonas aeruginosa* · Twitching motility

Introduction

Optogenetics, an important branch of synthetic biology (Cameron et al. 2014; Deisseroth 2010), is an excellent tool for rapid, noninvasive, and targetable cell manipulations with precise spatiotemporal resolution. Features of light and optogenetic reagents enable the use of such technology. In contrast with chemical molecules, light is highly tunable, noninvasive, exhibits no or low toxicity, and enables spatial precision, thereby avoiding the pleiotropic effects of small-molecule inducers. Optogenetic reagents comprise photosensory proteins that can transform the light signal into biochemical outputs (Brown et al. 2018; Rockwell and Lagarias 2010; Zhang et al. 2011). The two elements together enable optical manipulations with spatiotemporal precision. The powerful capabilities of optogenetic manipulation are particularly advantageous to controlling well-defined events in specific cell types at specific times in intact systems, which enables the studies of cellular processes and events in the context of other processes and events dependently happening in the rest of the tissue, the organism, and the circumstance as a whole.

Optogenetics stems from neuroscience and has become a modern research tool providing neuroscientists with an unprecedented level of control in neurons and having changed the way neuroscience is conducted (Boyden et al. 2005; Yizhar et al. 2011). However, applying optogenetic

✉ Shuai Yang
shuai.yang@siat.ac.cn

✉ Fan Jin
fan.jin@siat.ac.cn

[1] Shenzhen Synthetic Biology Infrastructure, Shenzhen Institute of Synthetic Biology, Shenzhen Institutes of Advanced Technology, Chinese Academy of Sciences, Shenzhen 518055, China

[2] CAS Key Laboratory of Quantitative Engineering Biology, Shenzhen Institute of Synthetic Biology, Shenzhen Institutes of Advanced Technology, Chinese Academy of Sciences, Shenzhen 518055, China

[3] West China School of Medicine, West China Hospital, Sichuan University, Chengdu 610041, Sichuan, China

Published online: 21 September 2022

tools reaches beyond neuroscience (Fenno et al. 2011) as these tools have already been applied to non-neuronal systems, such as prokaryotic cells (Fernandez-Rodriguez et al. 2017; Jin and Riedel-Kruse 2018; Levskaya et al. 2005, 2009; Olson et al. 2014a; Pu et al. 2018). The temporal precision provided by light is still crucial in these experiments, but the potential of the spatial resolution of light is not fully realized due to the most commonly used whole-field illumination (Fernandez-Rodriguez et al. 2017; Jin and Riedel-Kruse 2018; Pu et al. 2018). The unique property of light should be developed to the utmost. In other words, new technologies would be required to perform patterned or regional photo-stimulation, methods that could allow for the optical stimulation of defined cell types or localized cell regions to provide adequate cellular specificity. Previously, Leifer et al. described a real-time, multimodal illumination technology that makes optical control of neurons and muscles possible in the free-moving nematode *Caenorhabditis elegans* (Stirman et al. 2012, 2011). This targeted illumination technology offered a spatial resolution of 10 μm, suitable for projecting an illumination pattern onto small model organisms such as *C. elegans* (Guo et al. 2009; Leifer et al. 2011; Stirman et al. 2011), but did not apply to unicellular organisms sized at the sub-micron scale such as bacterial cells. This unmet need motivated us to develop a method for direct manipulation of various moving bacteria on a surface. Similarly, in this study, combining a high-throughput bacterial tracking algorithm and adaptive microscopy, we established a novel method, the adaptive tracking illumination (ATI) system. The ATI system with a spatial resolution of 0.61 μm could precisely and simultaneously illuminate single moving bacterial cells of interest through the in situ analysis and tracking of moving bacterial trajectories. Subsequently, we engineered *Pseudomonas aeruginosa* cells through the introduction of optogenetic modules and used the ATI system to optically manipulate these freely moving unicellular bacteria on a glass surface. The results showed that our ATI system allowed for the optogenetic gene expression control of specific cells with single-cell precision. Therefore, our newly established ATI system provides a strategy to perform real-time simultaneous illumination of multiple regions at the sub-micron scale, could be commonly used for optogenetic applications in bacteriology, and could further enhance our ability to investigate relevant pending problems using optogenetic methods.

Materials and methods

Multicolor optical path

The following optical path is similar to the 3D-SIM (Shao et al. 2011) approach, but prefers contrast for projection and in situ image switching. Similar optical paths were widely used in a super-resolution microscope (Huang et al. 2018; Kner et al. 2009). Therefore, we chose a fast ferroelectric spatial light modulator (SLM) (ForthDD, QXGA-R10), which can display binary bit-planes in real-time at high frequencies. The SLM is illuminated by a 24 × 24-mm collimated laser beam, reflecting from a polarizing beam splitting cube (Thorlabs PBS519, extinction ratio of T_p:T_s > 1000:1). The collimated laser beam is emerged from a multimode fiber and is expanded by a 10 × objective (Olympus, $NA = 0.4$). Before the light incident on the SLM, the collimated laser beam needs to be maintained in s-polarization through a reversing polarizing beam splitting cube (Thorlabs PBS251, extinction ratio 1000:1) in order to optimize the projection contrast (Fig. S1). The SLM can be used as an electronically defined optical phase grating: all pixels always reflect light but rotate the polarization depending on their ON or OFF state. When the pixel states are ON, the beam would switch to p-polarization, and consequently transmit through the polarizing beam splitting cube to form an illumination pattern. The pattern size eventually matches that of the camera chip using expanded achromatic lenses group (Thorlabs, TTL165-A, TTL180-A).

Ideally, when the pixel state of SLM is "ON," the intensity I_1 of the pixel at the image plane is calculated as below:

$$I_1 = I_s \times R_s \times f \times T_p + I_p \times R_p \times f \times T_s \quad (1)$$

where I_s and I_p are the amplitude of the s-polarization component and p-polarization component of the light beam. f is the reflectance of SLM. R_s and R_p are the reflectance of PBS to the s-polarization component and p-polarization component of the light beam. T_s and T_p are the transmittance of PBS to the s-polarization component and p-polarization component of the light beam. When the pixel state of SLM is "OFF," the intensity I_0 of the pixel at the image plane is calculated as below,

$$I_0 = I_s \times R_s \times f \times T_s + I_p \times R_p \times f \times T_p \quad (2)$$

Contrast c could be calculated by the equation below,

$$c = \frac{T_p}{T_s} - \frac{\left(\frac{T_p}{T_s}\right)^2 - 1}{\frac{I_s}{I_p} \times \frac{R_s}{R_p} + \frac{T_p}{T_s}} \quad (3)$$

The maximum contrast of projection is determined by the extinction ratio $T_p : T_s$. To optimize contrast of projection, the ratio of $I_s/I_p \times R_s/R_p$ should be large as possible.

The excitation light sources comprise a set of diode lasers (Coherent OBIS: 405–100 LX, 488–150 LX, 561–100 LS, 640–100 LX). The laser beams are collimated and coupled into the 10 m of a multimode fiber (Ceram Optec, core 200 × 200 μm) through collimated mirrors (Thorlabs,

PF10-03-G01) and a single-edge laser dichroic beamsplitter (Semrock, LM01-427–25, LM01-503–25, LM01-613–25, and LM01-659–25). The multimode fiber is coiled into a loop and is shook by a motor (Taobao), powered and triggered by low (< 5 V) and pulse voltage, respectively. Finally, the excitation light cleaned by a multi-band excitation filter (Chroma, ZET405/488/561/640VX2) is reflected onto the sample via one multi-band, imaging-quality beamsplitter (Chroma ZT405/488/561/640-phase R-UF3) and a 100×, 1.40 NA oil-immersion objective (Olympus UPlanSApo 100×/1.40 Oil). The fluorescent emission of the sample passes through the multi-band beamsplitter, notch filter (Semerock, NF03-405/488/561/635E-25), and emission filters in sequence. Then, it is eventually projected onto sCMOS cameras (Teledyne Photometrics, Prime BSI).

Processing system for in situ analysis and tracking

Bright-field (BF) images were obtained at a frame rate of 0.2 from the microscope. The image acquisition frame rate is sufficient for bacterial tracking of twitching motility, the dominating motility type of *P. aeruginosa* on the surface. BF images with background correction are stored in the CPU memory, except for those saved on the local hard drive. Two contiguity BF images in the memory are applied to image segmentation, cell recognition, and final bacterial tracking in MATLAB as previously reported (Jin et al. 2011; Xia et al. 2021). The major difference between the previously and hereby reported methods is in situ analysis and tracking in our novel approach (Fig. S2). Cell position and lineage are acquired in each frame. In the first frame, the target cells are designated or randomly generated. The target cells are then automatically tracked according to in situ cell tracking. Next, the projecting pattern (2048 × 1536) is generated by transforming the mask of the target cells in each frame (2048 × 2048) and sending them to SLM. Spatial transformation is inferred from control point pairs, calculated from the lattice mask of SLM and its corresponding snapped image in the camera.

System software and timing control

The entire setup is managed and run from a single computer, which in turn controls the camera computer via TCP/IP network links, the SLM via serial communication, and the microcontroller via HDMI communication. The required network connections are implemented using abstract client and server classes in MATLAB. The client and server do not need to be on different computers. This means that with sufficient computer performance, the entire setup can also be controlled from a single computer. The camera is connected to its core camera via Camera Link. The camera plugin includes the camera server and Java classes camera controller, which ultimately controls the camera using the interface provided by Micro-Manager. The cell tracking center runs a high-throughput bacterial tracking algorithm and transmits the mask of selected cells to the SLM. A microcontroller based on STM32H7 and AT24C512 controls the precise timing of the setup. It triggers the camera, the lasers, the motors, and the LED via digital I/O-lines, the piezo stage via analog I/O-lines, and is triggered by the LED output of FLCoS SLM so that each individual device performs the action previously determined via ATI at the right time.

When the command "snap image" is sent, the controller receives the first rising edge of the red LED signal, and then sends TTL sequences of the camera and laser. The camera operates in a "roll shutter" mode, meaning that the speed of current sCMOS chips depends on the number of lines to be read from the chip. The chip in use here runs at 11.2 µs (HDR mode) or 7.74 µs (11-bit) per line. As the camera exposure and readout are overlapped and accomplished by beginning the exposure row by row, real laser beam exposure would begin after the last line of exposure begins (approximately 24 ms, HDR mode), as shown in the diagram "Laser 488 nm." The TTL sequence of the laser is generated by V-sync of SLM "and" logical operation of the channel. The timing is carefully adjusted on the microcontroller: a digital storage oscilloscope is used to monitor the TTL signals from the microcontroller.

Stains and growth conditions

Pseudomonas aeruginosa strain PAO1 in this study was kindly provided by J. D. Shrout (University of Notre Dame). This strain is deposited in the American Type Culture Collection as ATCC 15,692. Table S1 summarizes the bacterial strains and plasmids used in this study. Additional details for optogenetics and reporter strain constructions are provided in the Supplementary methods. The strains were grown on LB agar plates at 37 °C for 24 h. Monoclonal colonies were inoculated and cultured in a minimal medium (FAB) at 37 °C with 30 mM glutamate as a carbon source under aerobic conditions, with the composition as follows per liter: $(NH_4)_2SO_4$, 2 g/L; $Na_2HPO_4 \cdot 12H_2O$, 12.02 g/L; KH_2PO_4, 3 g/L; NaCl, 3 g/L; $MgCl_2$, 93 g/mL; $CaCl_2 \cdot 2H_2O$, 14 g/mL; $FeCl_3$, 1 uM; and trace metals solution ($CaSO_4 \cdot 2H_2O$, 200 mg/L; $MnSO_4 \cdot 7H_2O$, 200 mg/L; $CuSO_4 \cdot 5H_2O$, 20 mg/L; $ZnSO_4 \cdot 7H_2O$, 20 mg/L; $CoSO_4 \cdot 7H_2O$, 10 mg/L; $NaMoO_4 \cdot H_2O$, 10 mg/L; H_3BO_3, 5 mg/L) 1 mL/L. The strains were harvested at $OD_{600} = 2.1$, and the bacterial cultures were further diluted (1:100) in fresh FAB mediums to culture to $OD_{600} = 0.4$ before use.

Gene expression manipulation in single cells

The bacterial strain (PAO1-pDawn-sfGFP) was inoculated into a flow cell (Denmark Technical University) and continuously cultured at 30 °C ± 0.1 °C in a flowing FAB medium (3.0 mL • h^{-1}) (Heydorn et al. 2000). We used an inverted fluorescent microscope (Olympus, IX81) equipped with a 100 × oil objective and an sCMOS camera to collect BF or fluorescent images at 15 s/frame or 30 min/frame, respectively. The fluorescent emission of sfGFP was triggered by the excitation of a 480-nm laser beam (Coherent) and passed a single-band emission filter (Semrock, 520/28 nm). The cells were selected at the first frame, then adaptive-tracked to be manipulated using ATI with a power density of 0.04 mW cm^{-2}. The power density of the manipulation lights was determined by measuring the power at the outlet of the objective using a power meter (Newport 842-PE).

Guiding biofilm formation using ATI

The bacterial strains of PAO1-*bphS*-EGFP and PAO1-*bphS*-mCherry were mixed at a ratio of 1:1 and inoculated into the modified flow cell for continuous culture at 30 °C ± 0.1 °C by flowing FAB medium (3.0 mL • h^{-1}). The cells with green or red fluorescence were selected to be manipulated using ATI with a power density of 0.05 mW·cm^{-2} during the first 10 h. Afterward, the flow cell contained the distinctive young biofilms were continuously cultured for up to 3 days in the dark to allow these young biofilms to mature. Finally, a laser-scan confocal microscope (Olympus FV1000) equipped with a 100 × oil objective was used to image the cell organizations as well as the three-dimensional (3D) structures of the mature biofilms using *z*-axis scanning (0.5 μm per step). The confocal images acquired at the different *z*-positions were used to reconstruct the structure of mature biofilms using ImageJ.

Results

The ATI system enables precise illumination of single bacterial cells

Figure 1a presents our adaptive tracking illumination system composed of two modules. First, it includes an integrated microscope with a structured illumination system for projecting to illuminate single cells. Second, it contains a signal processing system for in situ analysis and tracking the trajectories of moving bacteria. We used an inverted fluorescent microscope to set up the microscopic system for ATI. The structured illumination system includes (1) fiber-coupled laser sources (lasers at wavelengths of 488, 561, and 640 nm, coupled into a multimode fiber through a 4 × objective, and the multimode fiber is shaken by an electric motor to uniform the light intensity on the image plane); (2) a pattern of the SLM is projected into the field of the microscope, and the light pattern is precisely illuminated to the single bacterial scale; and (3) an additional 850-nm LED light is coupled to the illumination optical path for BF illuminations. The inverted fluorescent microscope equipped with a 100 × oil objective and an sCMOS camera is used to collect BF images with customized frequency. The acquired BF images are subjected to the signal processing system to track multiple single cells and obtain their information in real-time (Figs. 1b and S2). The masks of the selected cells are instantly sent to the SLM that is directly controlled by a commercial desktop through an HDMI port to generate a projection mask as a primary illumination image (2048 × 1560 pixels). The projection lights are generated by the fiber-coupled laser sources and remained polarized by passing through a polaroid before reaching the SLM. The primary illumination pattern is transferred through an amplification, a tube lens, a multi-band pass filter, and a dichroic mirror to form a demagnified illumination pattern at the focal plane of the objective of an inverted microscope. The objects of interest (e.g., freely moving bacterial cells) are also located and illuminated at the sample plane. To examine the projection resolution, we projected a sequence of different-sized demo patterns using our ATI system (Fig. 1c). The resulting patterns show the spatial resolution of the micro-projection reaching up to 0.61 μm (Fig. 1d) that is smaller than the length of single cells (about 2 μm for *P. aeruginosa* cells), thereby meeting the need of illumination of single bacterial cells. In addition, the ATI system has an extinction ratio of 200:1 (Fig. 1c and d), enabling a high contrast that can be used for gene expression light activation or silencing using optogenetics.

Synchronization of the ATI system

To ensure the synchronization of the ATI method, the system components are controlled by MATLAB codes and micro-manager and triggered precisely by a low-cost microcontroller that enables synchronous work (Fig. 2a). As the ferroelectric spatial light modulator is a central component in multiple recent SLM-based SIM setups, we also chose SLM-based projection and illumination. High-contrast projection could only be achieved by careful and exact synchronization between the SLM, as well as the cameras and light sources. We selected a sequence timing of 100 Hz and 8-bit depth provided by the manufacturers as basic timing. When the operation command "snap image" is sent, the first rising edge of the red LED pulse in the sequence is captured by the microcontroller (Fig. 2b). Then the microcontroller would send each TTL sequence simultaneously to trigger the operation of the devices. The motor (active high), camera

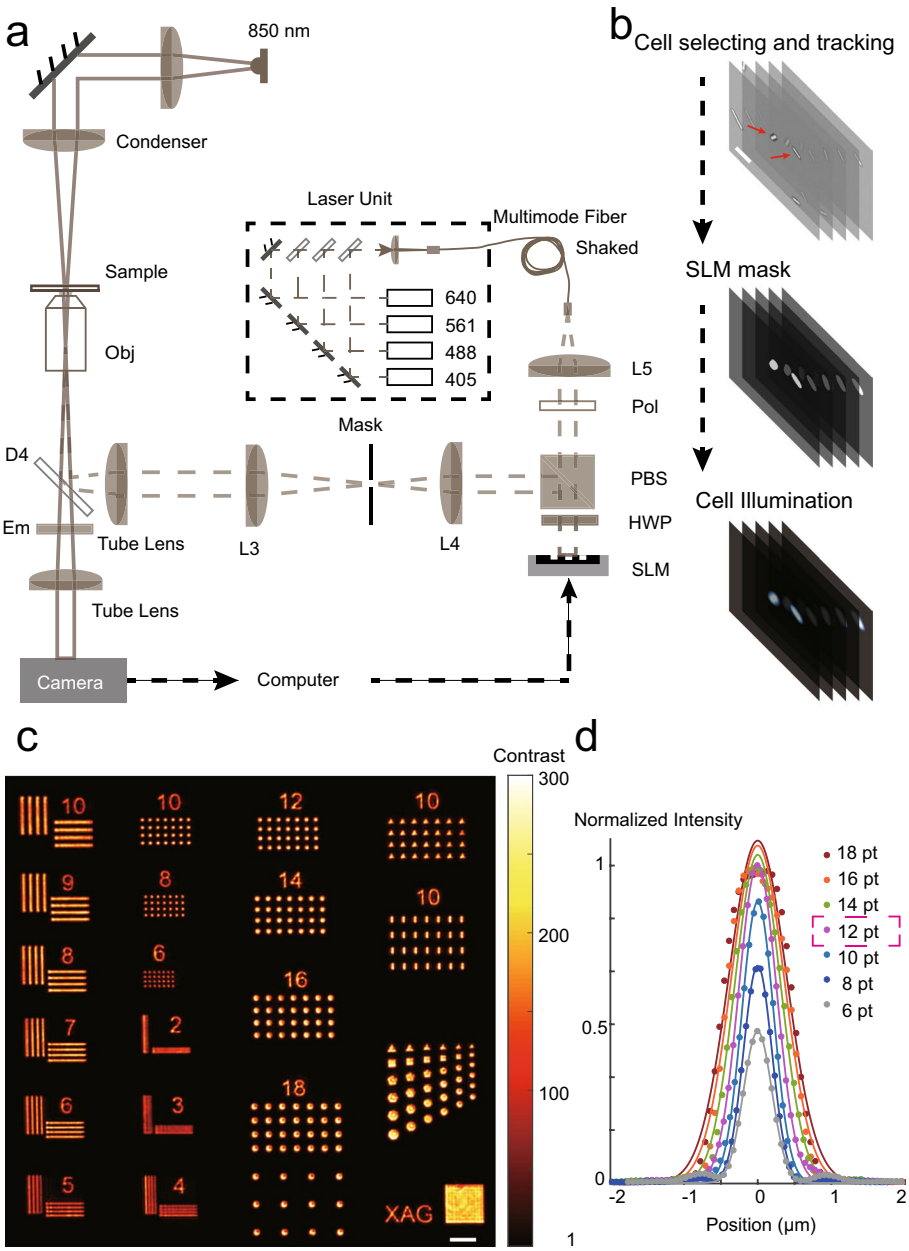

Fig. 1 Using adaptive tracking illuminations (ATI) to specifically illuminate single cells on the surface. **a** Schematic drawing of the ATI system. **b** A high-throughput bacterial tracking algorithm was applied for analyzing cell behaviors in real-time and the cell tracking masks were immediately fed back to an adaptive microscope equipped with a fast spatial light modulator (SLM). Eventually, adaptive illumination of the cells was achieved at a single-cell level. **c** A demo image with different sizes of patterns was projected using our ATI system. **d** Optical resolution of the ATI system, provided by projecting different pixels of a circle as shown in (**c**). A circular disc with a diameter of 12 pixels illuminated by a laser beam shows the maximal contrast and the most suitable resolution. Scale bar for all images: 5 μm

(active rising edge), LED (active high), laser (active high), and SLM are all triggered by TTL sequences sent from the microcontroller. The lasers are triggered by signals defined by the channels "and" LED pulse of the SLM. Here, "and" refers to logic gates and operations (Fig. 2b).

Spatial activation of gene expression in freely moving unicellular bacteria

To demonstrate the potential utility of our system, we applied an optimized optogenetic module, pDawn-Tn7, exploiting a blue light photoreceptor, to test the spatial gene expression activation in *P. aeruginosa* (Pu et al. 2018). We used a green fluorescent protein, sfGFP, as the reporter of light response with blue light–activated expression. That is, blue light–illuminated cells exhibit an increased GFP expression, and the intensity of GFP fluorescence can be computed to indicate the light response. Cells carrying the above-described optogenetic circuits were growing and freely moving on the glass surface of a flow cell. We randomly selected parts of cells in one image window (2048 × 2048 pixel) and illuminated them along with their offspring using 0.04-mW cm^{-2} and 488-nm light. Figure 3a shows that feedback illuminations could generate projected patterns to precisely track real-time cell movements or single-cell divisions (Supplementary Movie S1). We then examined

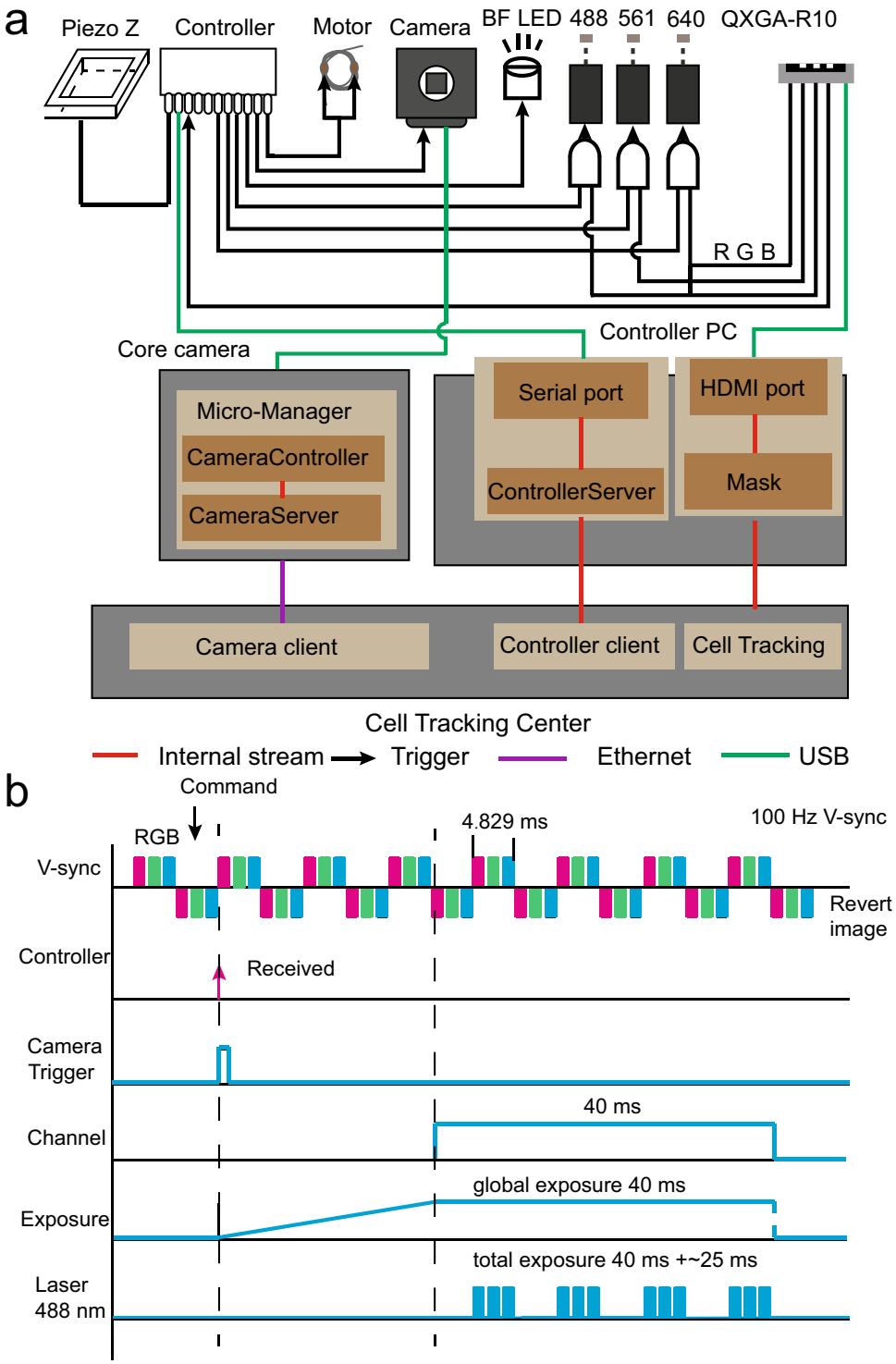

Fig. 2 Schematic overview of the control and timing diagram. **a** The control flow diagram shows system components receiving both real-time timing pulses (TTL) and network-based control commands. For more information, refer to the Supplementary Materials. **b** Timing diagram for the blue color (488 nm), 100 Hz V-sync of SLM, and 40-ms exposure mode with Prime BSI cameras (2048 rows) to snap images of channel "GFP" excited by a 488-nm laser beam

the fluorescence intensity evolution over time in single cells (Supplementary Movie S2). The results showed that the fluorescent intensity of the illuminated cells increased with time changing from 5 (0 h) to 108 (8 h) (Fig. 3b and d), while the fluorescent intensity of non-illuminated cells remained nearly constant (Fig. 3c and d), indicating the light activation of gene expression in specific cells. We prepared the representative genealogical tree of an illuminated (Fig. 3b) and a non-illuminated cell (Fig. 3c), where the GFP expression of the daughter cells is color-coded along each lineage, representing the single-cell spatial precision of our system. In addition, we did not observe any significant difference in the growth rate between the illuminated and non-illuminated cells ($p = 0.8$, Fig. 3d), indicating that the illumination light

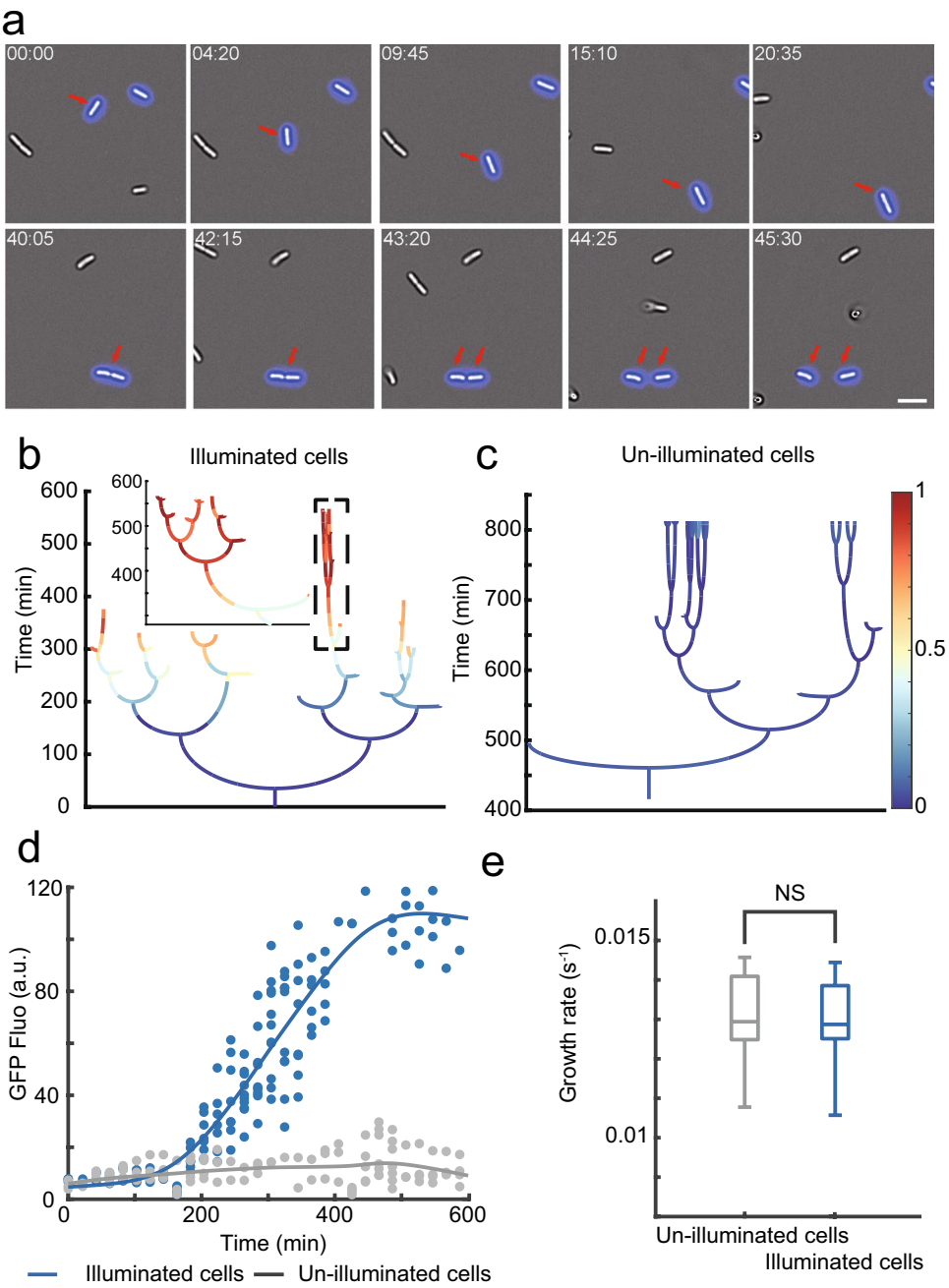

Fig. 3 By introducing optogenetic modules, the ATI system can precisely manipulate gene expression at a single-cell level. **a** A target cell being tracked and projected in real-time. The feedback illuminations can generate projected patterns to precisely follow the moving cells (the first parallel) and the daughter cells after the division of a cell of interest (the second parallel). **b**, **c** The fluorescent level from a mother cell, depicted by the genealogical tree of an illuminated cell (**b**) and a non-illuminated cell. **c** Color map representing the expression level of a fluorescent protein, sfGFP. **d** The fluorescent intensity of illuminated cells increased prominently but the fluorescent intensity of non-illuminated cells remained constant. **e** There was no significant difference in growth rate between illuminated and non-illuminated cells. The data were analyzed and obtained from 300 to 600 min. Scale bar for all images: 5 μm

was barely phototoxic. Taken together, these results suggest that, combined with the optogenetic modules, our ATI system displays the capacity of precise gene expression regulation at the single-cell level.

ATI enables biofilm formation guidance in *P. aeruginosa*

Due to the light-related advantages, the optogenetic modules exhibit the capacity of controlling biologically relevant cellular processes. Next, we aimed to manipulate bacterial behaviors, such as biofilm formation, with spatial and single-cell resolution. We incorporated an optogenetic part into the *P. aeruginosa* chromosome using the mini-CTX system. This optogenetic module encodes a heme oxygenase (bphO) and c-di-GMP diguanylate cyclase (bphS) that can cyclize two GTP molecules to form a c-di-GMP molecule in the presence of near-infrared light (Ryu and Gomelsky 2014), thereby enabling the direct manipulation of intracellular c-di-GMP levels upon illumination at 640 nm (0.05 mW·cm^{-2}). The c-di-GMP level increase represses the type IV pili-mediated twitching motility

and microcolony formation of single cells (Fig. 4a and b), thereby providing the potential for guiding biofilm formation. Then, we labeled the optogenetically modified cells using a green or red fluorescent protein (EGFP or mCherry). We co-cultured these differently labeled cells in a flow cell to facilitate their biofilm formation, during which we only selected GFP- or RFP-labeled cells and manipulated them by ATI in the first 10 h. Our results indicated that ATI enabled the selected cells (GFP- or RFP-labeled cells) and their offspring to form microcolonies in advance (Fig. 4c), whereas the unselected cells were distributed around the formed microcolonies (Fig. 4d). This result was in sharp contrast to that obtained for GFP- plus RFP-labeled cells without ATI treatment (Fig. S3). Thereafter, we continuously cultured (up to 72 h) these young biofilms with a distinct organization of cells in the dark to allow their maturation. These distinct young biofilms developed to mature biofilms possessing a distinct spatial organization of GFP- (Fig. 4e) or RFP-labeled cells (Fig. 4f). These results revealed that cell manipulation by ATI during early-stage biofilm formation enabled biofilm formation guidance.

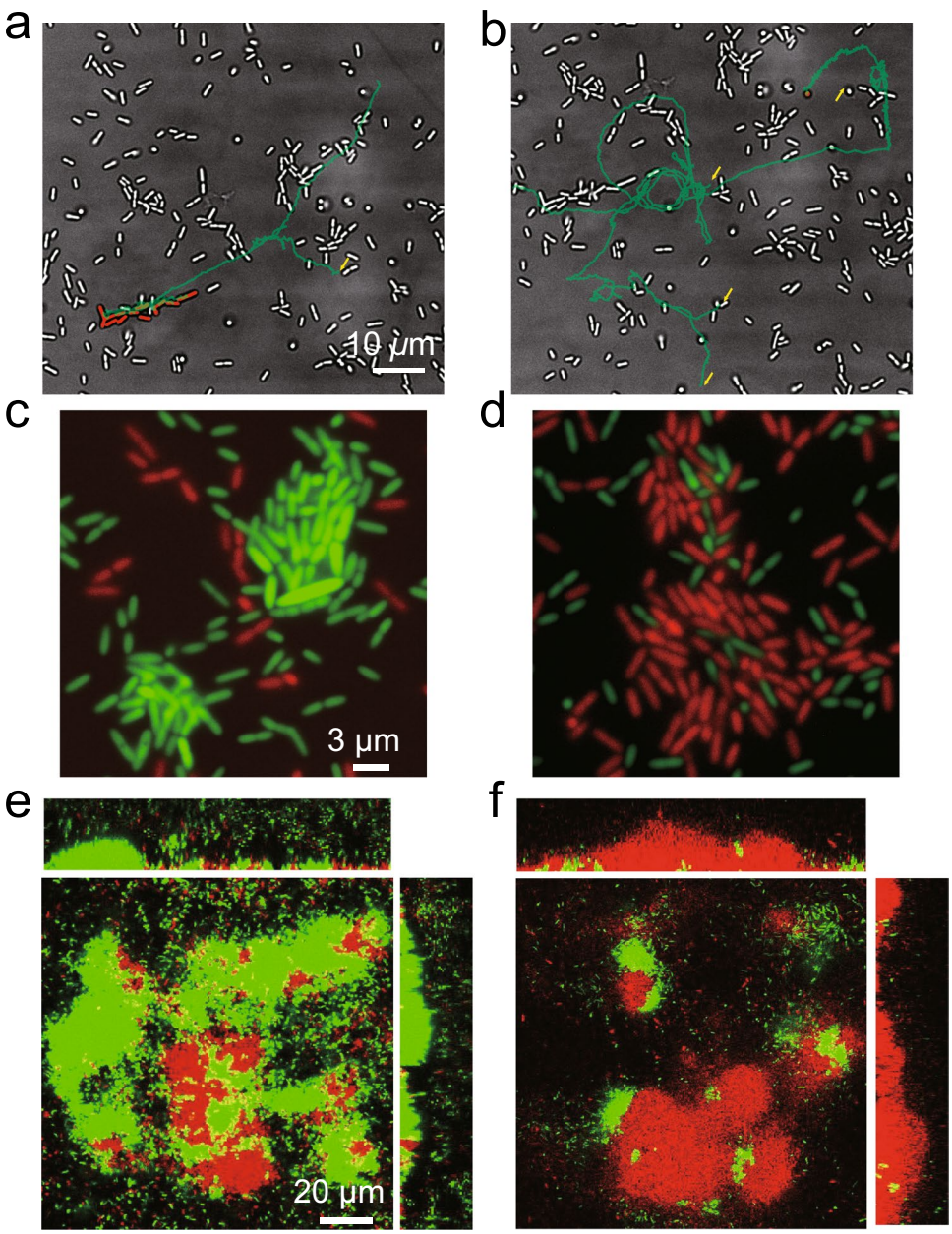

Fig. 4 Biofilm formation guidance using ATI in *P. aeruginosa*. **a** ATI enables selected cells and their offspring to form microcolonies in advance, compared with non-illuminated cells. **b** The lines represent bacterial movement traces. **c**, **d** Optogenetically modified cells labeled with a green or red fluorescent protein (EGFP or mCherry) were used for biofilm cultivation in a flow cell. **c** EGFP-labeled cells were manipulated by ATI; **d** mCherry-labeled cells were selected for manipulation. The fluorescence image was attained in the flow cell at the same time point at approximately t ~ 14 h. **e**, **f** The corresponding mature biofilm structure in (**c**, **d**) after 3 days of culture. The selected GFP- or the RFP-labeled cells possess distinctive spatial biofilm organizations

Discussion

In this study, we developed the ATI system that allows for tracking specific moving bacterial cells and performing precise spatial control of bacterial gene expression following cell modifications using an optogenetic circuit. In addition to the hereby presented experiments, in systems using two or more optogenetic modules with non-overlapping activation spectra, the illumination system can be easily expanded to adapt it to different optogenetic reagents using different scientific light sources. For instance, three-color lasers would allow the achievement of simultaneous and orthogonal RGB illumination without any switching between colors. Furthermore, our ATI system is easy to assemble and adapt by other researchers as (1) the hardware used to build the ATI system could consist of a commercial projector and an LED controller, which are quite common and inexpensive as we previously reported (Armbruster et al. 2019); (2) the optical setup of the ATI system is compatible with that of other commonly used microscopic techniques, including fluorescence, confocal, or even SLM-based SIM super-resolution approaches; (3) the software and algorithms used in ATI system, including image processing, single-cell tracking, and phenotype analysis, are modified rather flexibly; and (4) the wavelengths in ATI can be easily expanded to multiple colors to adapt them to different optogenetic tools (Ohlendorf et al. 2012; Olson et al. 2014b; Ryu et al. 2017). These factors allow researchers to simply integrate the ATI setup into their microscope and quickly modify the algorithms to track single cells with phenotypes of their interest, thereby markedly prompting studies of optogenetic tools. With these adaptions and optimizations, we also envision that the ATI system might be applied to answer various questions or resolve problems in microbiology.

Notably, the time required for data processing limits the application of ATI for investigating a quickly evolving biosystem or cellular process. For example, the data processing of a live image (using a commercial desktop equipped with an intel i7 CPU) in the present study typically took 3 s, limiting the use of ATI for manipulating rapidly swimming bacteria that can typically move at velocities reaching tens of microns per second. In addition to the data processing speed, the tracking algorithm accuracy limits the application of ATI for investigating microbes with high cell densities. For example, the current ATI cannot be used to manipulate the phenotypes of single cells during middle-stage biofilm formation as the algorithm cannot accurately track single cells in a dense microcolony. Developing new tracking algorithms or using powerful computers can address these limitations, thereby considerably expanding ATI applications.

Supplementary Information The online version contains supplementary material available at https://doi.org/10.1007/s00253-022-12177-6.

Acknowledgements We thank A. Möglich who provided the optogenetics plasmid.

Author contribution AG.X and RR.Z contributed equally to this work. F.J., S.Y, and AG.X conceived the project. AG.X established the ATI. AG.X, RR.Z, and S.Y performed the experiments. YJ.H, L.N, and L.P prepared the bacterial strain. Y.L helped prepare the synchronous control system. A.G and S.Y contributed jointly to data interpretation. A.G, S.Y, and F.J. contributed to the manuscript preparation. All authors reviewed the manuscript.

Funding This work was supported by the National Key Research and Development Program of China (Grant No. 2020YFA0906900 and 2018YFA0902700), the Scientific Instrument Developing Project of the Chinese Academy of Sciences (Grant No. YJKYYQ20200033), and the National Natural Science Foundation of China (Grant No. 32000060 to AG.X) (Grant No. 21774117 to F.J) (Grant No. 31901028 to S.Y).

Data availability The data sets generated during the current study are available from the corresponding author on reasonable request.

Declarations

Ethics approval This article does not contain any studies with human participants or animals performed by any of the authors.

Conflict of interest The authors declare no competing interests.

References

Armbruster CR, Lee CK, Parker-Gilham J, Anda J, Xia de A, Zhao K, Murakami K, Tseng BS, Hoffman LR, Jin F, Harwood CS, Wong GCL, Parsek MR (2019) Heterogeneity in surface sensing suggests a division of labor in Pseudomonas aeruginosa populations. Elife 8:e45084. https://doi.org/10.7554/eLife.45084

Boyden ES, Zhang F, Bamberg E, Nagel G, Deisseroth K (2005) Millisecond-timescale, genetically targeted optical control of neural activity. Nat Neurosci 8:1263–1268. https://doi.org/10.1038/nn1525

Brown J, Behnam R, Coddington L, Tervo DGR, Martin K, Proskurin M, Kuleshova E, Park J, Phillips J, Bergs ACF, Gottschalk A, Dudman JT, Karpova AY (2018) Expanding the optogenetics toolkit by topological inversion of rhodopsins. Cell 175:1131-1140.e1111. https://doi.org/10.1016/j.cell.2018.09.026

Cameron DE, Bashor CJ, Collins JJ (2014) A brief history of synthetic biology. Nat Rev Microbiol 12:381. https://doi.org/10.1038/nrmicro3239

Deisseroth K (2010) Optogenetics. Nat Methods 8:26. https://doi.org/10.1038/nmeth.f.324

Fenno L, Yizhar O, Deisseroth K (2011) The development and application of optogenetics. Annu Rev Neurosci 34:389–412. https://doi.org/10.1146/annurev-neuro-061010-113817

Fernandez-Rodriguez J, Moser F, Song M and Voigt CA (2017) Engineering RGB color vision into *Escherichia coli*. Nat Chem Biol 13:706. https://doi.org/10.1038/nchembio.2390, https://www.nature.com/articles/nchembio.2390#supplementary-information

Guo ZV, Hart AC and Ramanathan S (2009) Optical interrogation of neural circuits in *Caenorhabditis elegans*. Nat Methods 6:891–896. https://doi.org/10.1038/nmeth.1397

Heydorn A, Ersboll BK, Hentzer M, Parsek MR, Givskov M, Molin S (2000) Experimental Reproducibility in Flow-Chamber Biofilms Microbiol-Uk. Microbiology 146:2409–2415

Huang XS, Fan JC, Li LJ, Liu HS, Wu RL, Wu Y, Wei LS, Mao H, Lal A, Xi P, Tang LQ, Zhang YF, Liu YM, Tan S, Chen LY (2018) Fast long-term super-resolution imaging with Hessian structured illumination microscopy. Nat Biotechnol 36(5):451–459. https://doi.org/10.1038/nbt.4115

Jin F, Conrad JC, Gibiansky ML, Wong GCL (2011) Bacteria use type-IV pili to slingshot on surfaces. Proc Natl Acad Sci USA 108:12617–12622. https://doi.org/10.1073/pnas.1105073108

Jin X, Riedel-Kruse IH (2018) Biofilm lithography enables high-resolution cell patterning via optogenetic adhesin expression. Proc Natl Acad Sci USA 115:3698. https://doi.org/10.1073/pnas.1720676115

Kner P, Chhun BB, Griffis ER, Winoto L, Gustafsson MGL (2009) Super-resolution video microscopy of live cells by structured illumination. Nat Methods 6:339–342. https://doi.org/10.1038/nmeth.1324

Leifer AM, Fang-Yen C, Gershow M, Alkema MJ and Samuel ADT (2011) Optogenetic manipulation of neural activity in freely moving *Caenorhabditis elegans*. Nat Methods 8:147–152. https://doi.org/10.1038/nmeth.1554

Levskaya A, Chevalier AA, Tabor JJ, Simpson ZB, Lavery LA, Levy M, Davidson EA, Scouras A, Ellington AD, Marcotte EM and Voigt CA (2005) Synthetic biology: engineering *Escherichia coli* to see light. Nature 438:441–442

Levskaya A, Weiner OD, Lim WA and Voigt CA (2009) Spatiotemporal control of cell signalling using a light-switchable protein interaction. Nature 461:997–1001

Ohlendorf R, Vidavski RR, Eldar A, Moffat K, Moglich A (2012) From dusk till dawn: one-plasmid systems for light-regulated gene expression. J Mol Biol 416:534–542. https://doi.org/10.1016/j.jmb.2012.01.001

Olson EJ, Hartsough LA, Landry BP, Shroff R, Tabor JJ (2014a) Characterizing bacterial gene circuit dynamics with optically programmed gene expression signals. Nat Methods 11:449–455. https://doi.org/10.1038/nmeth.2884

Olson EJ, Hartsough LA, Landry BP, Shroff R, Tabor JJ (2014) Characterizing bacterial gene circuit dynamics with optically programmed gene expression signals. Nat Methods 11(4):449–455. https://doi.org/10.1038/nmeth.2884

Pu L, Yang S, Xia A, Jin F (2018) Optogenetics manipulation enables prevention of biofilm formation of engineered *Pseudomonas aeruginosa* on surfaces. ACS Synth Biol 7:200–208. https://doi.org/10.1021/acssynbio.7b00273

Rockwell NC, Lagarias JC (2010) A brief history of phytochromes. ChemPhysChem 11:1172–1180. https://doi.org/10.1002/cphc.200900894

Ryu M-H, Fomicheva A, Moskvin OV, Gomelsky M (2017) Optogenetic module for dichromatic control of c-di-GMP signaling. J Bacteriol. https://doi.org/10.1128/jb.00014-17

Ryu M-H, Gomelsky M (2014) Near-infrared light responsive synthetic c-di-GMP module for optogenetic applications. ACS Synth Biol 3:802–810. https://doi.org/10.1021/sb400182x

Shao L, Kner P, Rego EH, Gustafsson MGL (2011) Super-resolution 3D microscopy of live whole cells using structured illumination. Nat Methods 8:1044–1046. https://doi.org/10.1038/nmeth.1734

Stirman JN, Crane MM, Husson SJ, Gottschalk A and Lu H (2012) A multispectral optical illumination system with precise spatiotemporal control for the manipulation of optogenetic reagents. Nat Protoc 7:207–220. https://doi.org/10.1038/nprot.2011.433

Stirman JN, Crane MM, Husson SJ, Wabnig S, Schultheis C, Gottschalk A and Lu H (2011) Real-time multimodal optical control of neurons and muscles in freely behaving *Caenorhabditis elegans*. Nat Methods 8:153–158. https://doi.org/10.1038/nmeth.1555

Xia A, Qian M, Wang C, Huang Y, Liu Z, Ni L, Jin F (2021) Optogenetic modification of *Pseudomonas aeruginosa* enables controllable twitching motility and host infection. ACS Synth Biol 10:531–541. https://doi.org/10.1021/acssynbio.0c00559

Yizhar O, Fenno Lief E, Davidson Thomas J, Mogri M, Deisseroth K (2011) Optogenetics in neural systems. Neuron 71:9–34. https://doi.org/10.1016/j.neuron.2011.06.004

Zhang F, Vierock J, Yizhar O, Fenno LE, Tsunoda S, Kianianmomeni A, Prigge M, Berndt A, Cushman J, Polle J, Magnuson J, Hegemann P, Deisseroth K (2011) The microbial opsin family of optogenetic tools. Cell 147:1446–1457. https://doi.org/10.1016/j.cell.2011.12.004